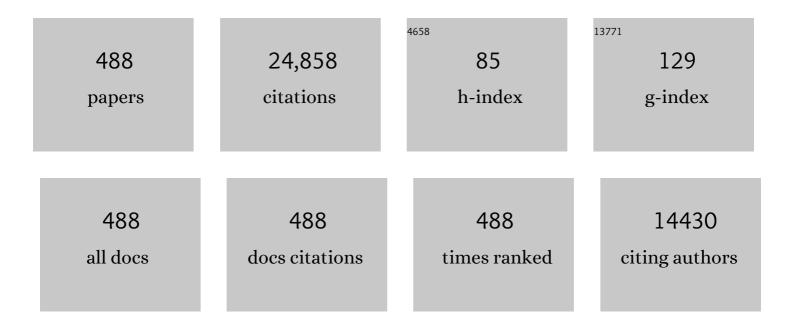
List of Publications by Year in descending order

Source: https://exaly.com/author-pdf/8795845/publications.pdf Version: 2024-02-01



ΙΙΔΝ ΖΗΔΝΟ

#	Article	IF	CITATIONS
1	Hybrid Zeolitic Imidazolate Frameworks with Catalytically Active TO ₄ Building Blocks. Angewandte Chemie - International Edition, 2011, 50, 450-453.	13.8	347
2	Homochiral Crystallization of Microporous Framework Materials from Achiral Precursors by Chiral Catalysis. Journal of the American Chemical Society, 2008, 130, 12882-12883.	13.7	319
3	Water-Stable Metal–Organic Frameworks for Fast and High Dichromate Trapping via Single-Crystal-to-Single-Crystal Ion Exchange. Chemistry of Materials, 2015, 27, 205-210.	6.7	295
4	Doping copper into ZIF-67 for enhancing gas uptake capacity and visible-light-driven photocatalytic degradation of organic dye. Journal of Materials Chemistry, 2012, 22, 21849.	6.7	289
5	Metal-organic frameworks based upon non-zeotype 4-connected topology. Coordination Chemistry Reviews, 2014, 261, 1-27.	18.8	286
6	A multifunctional helical Cu(i) coordination polymer with mechanochromic, sensing and photocatalytic properties. Chemical Communications, 2013, 49, 5660.	4.1	273
7	Synthetic strategies, diverse structures and tuneable properties of polyoxo-titanium clusters. Chemical Society Reviews, 2018, 47, 404-421.	38.1	272
8	Integrating the g-C ₃ N ₄ Nanosheet with B–H Bonding Decorated Metal–Organic Framework for CO ₂ Activation and Photoreduction. ACS Nano, 2018, 12, 5333-5340.	14.6	263
9	Multiroute Synthesis of Porous Anionic Frameworks and Size-Tunable Extraframework Organic Cation-Controlled Gas Sorption Properties. Journal of the American Chemical Society, 2009, 131, 16027-16029.	13.7	247
10	Design and synthesis of multifunctional metal–organic zeolites. Chemical Society Reviews, 2018, 47, 2130-2144.	38.1	243
11	Luminescent MTN -Type Cluster–Organic Framework with 2.6 nm Cages. Journal of the American Chemical Society, 2012, 134, 17881-17884.	13.7	239
12	Zeolitic Imidazolate Framework as Formaldehyde Gas Sensor. Inorganic Chemistry, 2014, 53, 5411-5413.	4.0	238
13	Chiral chemistry of metal–camphorate frameworks. Chemical Society Reviews, 2016, 45, 3122-3144.	38.1	229
14	Two-Dimensional Copper(I) Coordination Polymer Materials as Photocatalysts for the Degradation of Organic Dyes. Inorganic Chemistry, 2013, 52, 12-14.	4.0	228
15	Versatile Structureâ€Directing Roles of Deepâ€Eutectic Solvents and Their Implication in the Generation of Porosity and Open Metal Sites for Gas Storage. Angewandte Chemie - International Edition, 2009, 48, 3486-3490.	13.8	227
16	Zeolitic Boron Imidazolate Frameworks. Angewandte Chemie - International Edition, 2009, 48, 2542-2545.	13.8	224
17	A Simultaneous Redox, Alkylation, Self-Assembly Reaction under Solvothermal Conditions Afforded a Luminescent Copper(I) Chain Polymer Constructed of Cu3I4- and EtS-4-C5H4N+Et Components (Et =) Tj ETQq1	. 1 0 .3. 8431	.4 ജങ്ങ /Ovei
18	Enhanced photocatalytic hydrogen production activity via dual modification of MOF and reduced graphene oxide on CdS. Chemical Communications, 2014, 50, 8533.	4.1	212

#	Article	IF	CITATIONS
19	Synthesis, Structure, and Luminescent Properties of Hybrid Inorganicâ^'Organic Framework Materials Formed by Lead Aromatic Carboxylates: Inorganic Connectivity Variation from 0D to 3D. Inorganic Chemistry, 2009, 48, 6517-6525.	4.0	204
20	<i>In situ</i> synthesis of n–n Bi ₂ MoO ₆ & Bi ₂ S ₃ heterojunctions for highly efficient photocatalytic removal of Cr(<scp>vi</scp>). Journal of Materials Chemistry A, 2018, 6, 22580-22589.	10.3	200
21	Integrated Molecular Chirality, Absolute Helicity, and Intrinsic Chiral Topology in Three-Dimensional Open-Framework Materials. Journal of the American Chemical Society, 2008, 130, 17246-17247.	13.7	196
22	Isolated Squareâ€Planar Copper Center in Boron Imidazolate Nanocages for Photocatalytic Reduction of CO ₂ to CO. Angewandte Chemie - International Edition, 2019, 58, 11752-11756.	13.8	194
23	A 3.6 nm Ti ₅₂ –Oxo Nanocluster with Precise Atomic Structure. Journal of the American Chemical Society, 2016, 138, 7480-7483.	13.7	193
24	Multiple Functions of Ionic Liquids in the Synthesis of Threeâ€Dimensional Lowâ€Connectivity Homochiral and Achiral Frameworks. Angewandte Chemie - International Edition, 2008, 47, 5434-5437.	13.8	187
25	Tuning Structural Topologies of Three Photoluminescent Metal–Organic Frameworks via Isomeric Biphenyldicarboxylates. Inorganic Chemistry, 2012, 51, 9677-9682.	4.0	187
26	Hierarchical MoS ₂ Hollow Architectures with Abundant Mo Vacancies for Efficient Sodium Storage. ACS Nano, 2019, 13, 5533-5540.	14.6	187
27	An Ultrastable Europium(III)–Organic Framework with the Capacity of Discriminating Fe ²⁺ /Fe ³⁺ lons in Various Solutions. Inorganic Chemistry, 2016, 55, 10114-10117.	4.0	186
28	Acid and Base Resistant Zirconium Polyphenolateâ€Metalloporphyrin Scaffolds for Efficient CO ₂ Photoreduction. Advanced Materials, 2018, 30, 1704388.	21.0	184
29	Fullerene-like Polyoxotitanium Cage with High Solution Stability. Journal of the American Chemical Society, 2016, 138, 2556-2559.	13.7	183
30	Bandgap Engineering of Titanium–Oxo Clusters: Labile Surface Sites Used for Ligand Substitution and Metal Incorporation. Angewandte Chemie - International Edition, 2016, 55, 5160-5165.	13.8	181
31	Manganese and Magnesium Homochiral Materials:  Decoration of Honeycomb Channels with Homochiral Chains. Journal of the American Chemical Society, 2007, 129, 14168-14169.	13.7	180
32	Urothermal Synthesis of Crystalline Porous Materials. Angewandte Chemie - International Edition, 2010, 49, 8876-8879.	13.8	179
33	MOFâ€Templated Synthesis of Ultrasmall Photoluminescent Carbonâ€Nanodot Arrays for Optical Applications. Angewandte Chemie - International Edition, 2017, 56, 6853-6858.	13.8	179
34	A Tale of Three Carboxylates: Cooperative Asymmetric Crystallization of a Threeâ€Dimensional Microporous Framework from Achiral Precursors. Angewandte Chemie - International Edition, 2010, 49, 1267-1270.	13.8	172
35	Comparative Study of Homochiral and Racemic Chiral Metal-Organic Frameworks Built from Camphoric Acid. Chemistry of Materials, 2007, 19, 5083-5089.	6.7	166
36	Zeolite RHO-Type Net with the Lightest Elements. Journal of the American Chemical Society, 2009, 131, 6111-6113.	13.7	161

#	Article	IF	CITATIONS
37	Anionic Lanthanide MOFs as a Platform for Iron-Selective Sensing, Systematic Color Tuning, and Efficient Nanoparticle Catalysis. Inorganic Chemistry, 2017, 56, 1402-1411.	4.0	157
38	Cobalt Boron Imidazolate Framework Derived Cobalt Nanoparticles Encapsulated in B/N Codoped Nanocarbon as Efficient Bifunctional Electrocatalysts for Overall Water Splitting. Advanced Functional Materials, 2018, 28, 1801136.	14.9	155
39	Hydrothermal Syntheses, Crystal Structures, and Properties of a Novel Class of 3,3â€~,4,4â€~-Benzophenone-tetracarboxylate (BPTC) Polymers. Inorganic Chemistry, 2004, 43, 8085-8091.	4.0	153
40	Tunable MoS ₂ /SnO ₂ P–N Heterojunctions for an Efficient Trimethylamine Gas Sensor and 4-Nitrophenol Reduction Catalyst. ACS Sustainable Chemistry and Engineering, 2018, 6, 12375-12384.	6.7	151
41	Highly Selective and Sensitive Trimethylamine Gas Sensor Based on Cobalt Imidazolate Framework Material. ACS Applied Materials & Interfaces, 2014, 6, 22871-22875.	8.0	146
42	Water-Soluble and Ultrastable Ti ₄ L ₆ Tetrahedron with Coordination Assembly Function. Journal of the American Chemical Society, 2017, 139, 16845-16851.	13.7	145
43	Organic Cation and Chiral Anion Templated 3D Homochiral Openâ€Framework Materials with Unusual Squareâ€Planar {M ₄ (OH)} Units. Angewandte Chemie - International Edition, 2007, 46, 8388-8391.	13.8	143
44	Pore partition effect on gas sorption properties of an anionic metal–organic framework with exposed Cu2+ coordination sites. Chemical Communications, 2011, 47, 10647.	4.1	139
45	Engineering the Coordination Sphere of Isolated Active Sites to Explore the Intrinsic Activity in Single-Atom Catalysts. Nano-Micro Letters, 2021, 13, 136.	27.0	138
46	Chiralization of Diamond Nets: Stretchable Helices and Chiral and Achiral Nets with Nearly Identical Unit Cells. Angewandte Chemie - International Edition, 2007, 46, 6115-6118.	13.8	135
47	Interrupted Zeolite LTA and ATN-Type Boron Imidazolate Frameworks. Journal of the American Chemical Society, 2011, 133, 11884-11887.	13.7	134
48	Using alkaline-earth metal ions to tune structural variations of 1,3,5-benzenetricarboxylate coordination polymers. Dalton Transactions, 2013, 42, 2294-2301.	3.3	134
49	Topology Analysis and Nonlinear-Optical-Active Properties of Luminescent Metalâ^'Organic Framework Materials Based on Zinc/Lead Isophthalates. Inorganic Chemistry, 2008, 47, 8286-8293.	4.0	132
50	A Confined Fabrication of Perovskite Quantum Dots in Oriented MOF Thin Film. ACS Applied Materials & Interfaces, 2016, 8, 28737-28742.	8.0	132
51	Metal-organic frameworks for electrochemical reduction of carbon dioxide: The role of metal centers. Journal of Energy Chemistry, 2020, 40, 156-170.	12.9	130
52	Epitaxial growth of oriented prussian blue analogue derived well-aligned CoFe2O4 thin film for efficient oxygen evolution reaction. Applied Catalysis B: Environmental, 2019, 245, 1-9.	20.2	128
53	Host–Guest Chirality Interplay: A Mutually Induced Formation of a Chiral ZMOF and Its Double-Helix Polymer Guests. Journal of the American Chemical Society, 2016, 138, 786-789.	13.7	125
54	Water-Stable Metal–Organic Frameworks with Selective Sensing on Fe ³⁺ and Nitroaromatic Explosives, and Stimuli-Responsive Luminescence on Lanthanide Encapsulation. Inorganic Chemistry, 2019, 58, 1481-1491.	4.0	125

#	Article	IF	CITATIONS
55	Alkaline earth metal ion doped Zn(ii)-terephthalates. CrystEngComm, 2012, 14, 4843.	2.6	124
56	pH Influence on the Structural Variations of 4,4′-Oxydiphthalate Coordination Polymers. Crystal Growth and Design, 2012, 12, 333-345.	3.0	124
57	Epitaxial growth and applications of oriented metal–organic framework thin films. Coordination Chemistry Reviews, 2019, 378, 513-532.	18.8	122
58	A Polar Luminescent Zn Polymer Containing an Unusual Noninterpenetrated utp Net. Inorganic Chemistry, 2006, 45, 3161-3163.	4.0	121
59	Cluster-Organic Framework Materials as Heterogeneous Catalysts for High Efficient Addition Reaction of Diethylzinc to Aromatic Aldehydes. Chemistry of Materials, 2012, 24, 4711-4716.	6.7	121
60	Tuning a layer to a pillared-layer metal–organic framework for adsorption and separation of light hydrocarbons. Chemical Communications, 2013, 49, 11323.	4.1	121
61	Isomerism in Titaniumâ€Oxo Clusters: Molecular Anatase Model with Atomic Structure and Improved Photocatalytic Activity. Angewandte Chemie - International Edition, 2019, 58, 1320-1323.	13.8	121
62	Three-Dimensional Open Framework Built from Cuâ^'S Icosahedral Clusters and Its Photocatalytic Property. Journal of the American Chemical Society, 2008, 130, 15238-15239.	13.7	120
63	Surface step decoration of isolated atom as electron pumping: Atomic-level insights into visible-light hydrogen evolution. Nano Energy, 2018, 45, 109-117.	16.0	118
64	Recent Advances on Transition Metal Dichalcogenides for Electrochemical Energy Conversion. Advanced Materials, 2021, 33, e2008376.	21.0	114
65	Assembling Polyoxoâ€Titanium Clusters and CdS Nanoparticles to a Porous Matrix for Efficient and Tunable H ₂ â€Evolution Activities with Visible Light. Advanced Materials, 2017, 29, 1603369.	21.0	113
66	Lanthanide-Thiophene-2,5-dicarboxylate Frameworks: Ionothermal Synthesis, Helical Structures, Photoluminescent Properties, and Single-Crystal-to-Single-Crystal Guest Exchange. Inorganic Chemistry, 2012, 51, 523-530.	4.0	112
67	Synthetic design of functional boron imidazolate frameworks. Coordination Chemistry Reviews, 2016, 307, 255-266.	18.8	108
68	Chiral Semiconductor Frameworks from Cadmium Sulfide Clusters. Journal of the American Chemical Society, 2007, 129, 8412-8413.	13.7	107
69	Synthesis, Structure, and Physical Properties of a New Anions-Controlled Cd(II)-Guanazole (3,5-Diamino-1,2,4-triazole) Hybrid Family. Inorganic Chemistry, 2008, 47, 4861-4876.	4.0	107
70	Three-Dimensional Homochiral Transition-Metal Camphorate Architectures Directed by a Flexible Auxiliary Ligand. Inorganic Chemistry, 2008, 47, 3495-3497.	4.0	106
71	Tunable Synthesis of Hollow Metal–Nitrogen–Carbon Capsules for Efficient Oxygen Reduction Catalysis in Proton Exchange Membrane Fuel Cells. ACS Nano, 2019, 13, 8087-8098.	14.6	106
72	New Zeolitic Imidazolate Frameworks: From Unprecedented Assembly of Cubic Clusters to Ordered Cooperative Organization of Complementary Ligands. Chemistry of Materials, 2008, 20, 7377-7382.	6.7	102

#	Article	IF	CITATIONS
73	A new approach towards tetrahedral imidazolate frameworks for high and selective CO2 uptake. Chemical Communications, 2011, 47, 5828.	4.1	102
74	Highly active nonprecious metal hydrogen evolution electrocatalyst: ultrafine molybdenum carbide nanoparticles embedded into a 3D nitrogen-implanted carbon matrix. NPG Asia Materials, 2016, 8, e293-e293.	7.9	100
75	A Series of Ca(II) or Ba(II) Inorganic–Organic Hybrid Frameworks Based on Aromatic Polycarboxylate Ligands with the Inorganic M–O–M (M = Ca, Ba) Connectivity from 1D to 3D. Crystal Growth and Design, 2012, 12, 3231-3238.	3.0	99
76	Atomically Precise Multimetallic Semiconductive Nanoclusters with Optical Limiting Effects. Angewandte Chemie - International Edition, 2018, 57, 11252-11256.	13.8	99
77	Synthesis of a Boron–Imidazolate Framework Nanosheet with Dimer Copper Units for CO ₂ Electroreduction to Ethylene. Angewandte Chemie - International Edition, 2021, 60, 16687-16692.	13.8	99
78	Mesoporous Assembly of Aluminum Molecular Rings for Iodine Capture. Journal of the American Chemical Society, 2021, 143, 2325-2330.	13.7	98
79	Absolute helicity induction in three-dimensional homochiral frameworks. Chemical Communications, 2009, , 206-208.	4.1	96
80	Gas Sorption, Second-Order Nonlinear Optics, and Luminescence Properties of a Series of Lanthanide–Organic Frameworks Based on Nanosized Tris((4-carboxyl)phenylduryl)amine Ligand. Inorganic Chemistry, 2013, 52, 12758-12762.	4.0	96
81	Charge Matching on Designing Neutral Cadmium–Lanthanide–Organic Open Frameworks for Luminescence Sensing. Chemistry - an Asian Journal, 2012, 7, 1069-1073.	3.3	95
82	Highly Efficient CH Oxidative Activation by a Porous Mn ^{III} –Porphyrin Metal–Organic Framework under Mild Conditions. Chemistry - A European Journal, 2013, 19, 14316-14321.	3.3	95
83	Temperature dependent charge distribution in three-dimensional homochiral cadmium camphorates. Chemical Communications, 2008, , 444-446.	4.1	94
84	Supramolecular Isomerism and Various Chain/Layer Substructures in Silver(I) Compounds: Syntheses, Structures, and Luminescent Properties. Crystal Growth and Design, 2009, 9, 4884-4896.	3.0	93
85	A surface-mounted MOF thin film with oriented nanosheet arrays for enhancing the oxygen evolution reaction. Journal of Materials Chemistry A, 2019, 7, 18519-18528.	10.3	92
86	Role of molar-ratio, temperature and solvent on the Zn/Cd 1,2,4-triazolate system with novel topological architectures. CrystEngComm, 2011, 13, 3536.	2.6	89
87	Dynamic microporous indium(<scp>iii</scp>)-4,4′-oxybis(benzoate) framework with high selectivity for the adsorption of CO ₂ over N ₂ . Chemical Communications, 2011, 47, 770-772.	4.1	87
88	Homochiral metal–organic frameworks for enantioseparation. Chemical Society Reviews, 2021, 50, 5706-5745.	38.1	86
89	Interweaving 3D Network with Double Helical Tubes Filled by 1D Coordination Polymer Chains. Inorganic Chemistry, 2004, 43, 6525-6527.	4.0	85
90	Ionothermal Synthesis of Homochiral Framework with Acetate-Pillared Cobaltâ^'Camphorate Architecture. Inorganic Chemistry, 2008, 47, 5567-5569.	4.0	85

#	Article	IF	CITATIONS
91	Interpenetrated Metal-Porphyrinic Framework for Enhanced Nonlinear Optical Limiting. Journal of the American Chemical Society, 2021, 143, 17162-17169.	13.7	85
92	A 3-D Noninterpenetrating Diamondoid Network of a Decanuclear Copper(I) Complex. Inorganic Chemistry, 2005, 44, 3386-3388.	4.0	83
93	Chiral Porous Metacrystals: Employing Liquid-Phase Epitaxy to Assemble Enantiopure Metal–Organic Nanoclusters into Molecular Framework Pores. ACS Nano, 2016, 10, 977-983.	14.6	83
94	Multifunctional Homochiral Lanthanide Camphorates with Mixed Achiral Terephthalate Ligands. Inorganic Chemistry, 2010, 49, 9257-9264.	4.0	82
95	Induction in urothermal synthesis of chiral porous materials from achiral precursors. Chemical Communications, 2011, 47, 4950.	4.1	80
96	Tuning MOF Stability and Porosity via Adding Rigid Pillars. Inorganic Chemistry, 2012, 51, 9649-9654.	4.0	79
97	A New Zeolitic Topology with Sixteenâ€Membered Ring and Multidimensional Large Pore Channels. Chemistry - A European Journal, 2008, 14, 7771-7773.	3.3	76
98	Highly Selective Sorption of Small Hydrocarbons and Photocatalytic Properties of Three Metal–Organic Frameworks Based on Tris(4-(1 <i>H</i> -imidazol-1-yl)phenyl)amine Ligand. Inorganic Chemistry, 2014, 53, 4209-4214.	4.0	76
99	High Color Rendering Index White-Light Emission from UV-Driven LEDs Based on Single Luminescent Materials: Two-Dimensional Perovskites (C ₆ H ₅ C ₂ H ₄ NH ₃) ₂ PbBr <i>sub>x ACS Applied Materials & amp: Interfaces, 2018, 10, 15980-15987.</i>	800 <td>>Ċĺ⁵sub>4∂</td>	>Ċĺ ⁵ sub>4∂
100	Anion-Induced Coordination Versatility of 1H-1,2,4-Triazole-3-thiol (HtrzSH) Affording a New Hybrid System of Cadmium(II) Polymers: Synthesis, Structure, and Luminescent Properties. Crystal Growth and Design, 2008, 8, 2562-2573.	3.0	74
101	Organically templated metal–organic framework with 2-fold interpenetrated {33.59.63}-lcy net. Chemical Communications, 2008, , 2532.	4.1	74
102	Open diamondoid amino-functionalized MOFs for CO2 capture. Chemical Communications, 2012, 48, 4842.	4.1	74
103	A new approach towards zeolitic tetrazolate-imidazolate frameworks (ZTIFs) with uncoordinated N-heteroatom sites for high CO2uptake. Chemical Communications, 2014, 50, 12065-12068.	4.1	74
104	Hollow Cu–TiO ₂ /C nanospheres derived from a Ti precursor encapsulated MOF coating for efficient photocatalytic hydrogen evolution. Journal of Materials Chemistry A, 2018, 6, 7175-7181.	10.3	74
105	Cul Cluster-Based Organic Frameworks with Unusual 4- and 5-Connected Topologies. Crystal Growth and Design, 2011, 11, 29-32.	3.0	69
106	N-donor ligands enhancing luminescence properties of seven Zn/Cd(<scp>ii</scp>) MOFs based on a large rigid l€-conjugated carboxylate ligand. CrystEngComm, 2015, 17, 9155-9166.	2.6	69
107	Dual-Emission SG7@MOF Sensor via SC–SC Transformation: Enhancing the Formation of Excimer Emission and the Range and Sensitivity of Detection. ACS Applied Materials & Interfaces, 2018, 10, 18012-18020.	8.0	68
108	Auto-controlled fabrication of a metal-porphyrin framework thin film with tunable optical limiting effects. Chemical Science, 2020, 11, 1935-1942.	7.4	68

#	Article	IF	CITATIONS
109	Breaking the Mirror: pHâ€Controlled Chirality Generation from a <i>meso</i> Ligand to a Racemic Ligand. Chemistry - A European Journal, 2009, 15, 989-1000.	3.3	67
110	Unusual parallel entanglement of metal–organic 2D frameworks with coexistence of polyrotaxane, polycatenane and interdigitation. CrystEngComm, 2009, 11, 1030.	2.6	67
111	Stable Mg-Metal–Organic Framework (MOF) and Unstable Zn-MOF Based on Nanosized Tris((4-carboxyl)phenylduryl)amine Ligand. Crystal Growth and Design, 2013, 13, 6-9.	3.0	67
112	1D chain structure, NLO and luminescence properties of. Inorganic Chemistry Communication, 2004, 7, 1139-1141.	3.9	66
113	General Synthetic Strategy for Libraries of Supported Multicomponent Metal Nanoparticles. ACS Nano, 2018, 12, 4594-4604.	14.6	66
114	Interface engineered <i>in situ</i> anchoring of Co ₉ S ₈ nanoparticles into a multiple doped carbon matrix: highly efficient zinc–air batteries. Nanoscale, 2018, 10, 2649-2657.	5.6	66
115	In Situ Synthesis of Tetradentate Dye for Construction of Three-Dimensional Homochiral Phosphor. Chemistry of Materials, 2008, 20, 5457-5459.	6.7	63
116	Tuning structural topologies of four Ni(ii) coordination polymers through modifying the substitute group of organic ligand. CrystEngComm, 2013, 15, 6191.	2.6	63
117	Vertically Aligned MoS ₂ with In-Plane Selectively Cleaved Mo–S Bond for Hydrogen Production. Nano Letters, 2021, 21, 1848-1855.	9.1	63
118	A rare metal–organic 3D architecture with a pseudo-primitive cubic topology with double edges constructed from a 12-connected SBU. New Journal of Chemistry, 2005, 29, 995.	2.8	62
119	Surface modification of polyoxometalate host–guest supramolecular architectures: from metal–organic pseudorotaxane framework to molecular box. Chemical Communications, 2011, 47, 4150.	4.1	62
120	Large Titanium-Oxo Clusters as Precursors to Synthesize the Single Crystals of Ti-MOFs. , 2021, 3, 64-68.		62
121	Liquid-phase epitaxial growth of a homochiral MOF thin film on poly(<scp>l</scp> -DOPA) functionalized substrate for improved enantiomer separation. Chemical Communications, 2016, 52, 772-775.	4.1	60
122	Combining a Titanium–Organic Cage and a Hydrogenâ€Bonded Organic Cage for Highly Effective Thirdâ€Order Nonlinear Optics. Angewandte Chemie - International Edition, 2021, 60, 2920-2923.	13.8	59
123	Chemical Communications, 2004, , 1046.	4.1	58
124	Microporous Zinc Tris[(4-carboxyl)phenylduryl]amine Framework with an Unusual Topological Net for Gas Storage and Separation. Inorganic Chemistry, 2012, 51, 1995-1997.	4.0	58
125	A Highly Energetic Nâ€Rich Metal–Organic Framework as a New Highâ€Energyâ€Đensity Material. Chemistry - A European Journal, 2016, 22, 1141-1145.	3.3	58
126	Guest inducing fluorescence switching in lanthanide–tris((4-carboxyl)phenylduryl)amine frameworks integrating porosity and flexibility. Journal of Materials Chemistry C, 2014, 2, 4436.	5.5	57

#	Article	IF	CITATIONS
127	Ag ₁₀ Ti ₂₈ â€Oxo Cluster Containing Singleâ€Atom Silver Sites: Atomic Structure and Synergistic Electronic Properties. Angewandte Chemie - International Edition, 2019, 58, 10932-10935.	13.8	57
128	A new open framework material based on designed semi-rigid T-shaped tricarboxylate ligand. Inorganic Chemistry Communication, 2011, 14, 986-989.	3.9	56
129	Integration of rigid and flexible organic parts for the construction of a homochiral metal–organic framework with high porosity. Chemical Communications, 2015, 51, 2565-2568.	4.1	56
130	Epitaxial Growth of MOF Thin Film for Modifying the Dielectric Layer in Organic Field-Effect Transistors. ACS Applied Materials & Interfaces, 2017, 9, 7259-7264.	8.0	56
131	Conformation Preference of a Flexible Cyclohexanetetracarboxylate Ligand in Three New Metal-Organic Frameworks: Structures, Magnetic and Luminescent Properties. Inorganic Chemistry, 2009, 48, 7194-7200.	4.0	55
132	Redox-active Cu(<scp>i</scp>) boron imidazolate framework for mechanochromic and catalytic applications. Chemical Communications, 2014, 50, 8754.	4.1	55
133	Structural Diversity and Photoluminescent Properties of Zinc Benzotriazole-5-carboxylate Coordination Polymers. Inorganic Chemistry, 2014, 53, 1500-1506.	4.0	55
134	Cadmiumâ^'Porphyrin Coordination Networks: Rich Coordination Modes and Three-Dimensional Four-Connected CdSO4and (3,5)-Connected hms Nets. Crystal Growth and Design, 2007, 7, 2576-2581.	3.0	54
135	Nucleotide atalyzed Conversion of Racemic Zeoliteâ€₹ype Zincophosphate into Enantioenriched Crystals. Angewandte Chemie - International Edition, 2009, 48, 6049-6051.	13.8	54
136	Variable Lithium Coordination Modes in Two- and Three-Dimensional Lithium Boron Imidazolate Frameworks. Chemistry of Materials, 2009, 21, 3830-3837.	6.7	54
137	Interface Designing over WS ₂ /W ₂ C for Enhanced Hydrogen Evolution Catalysis. ACS Applied Energy Materials, 2018, 1, 3377-3384.	5.1	54
138	Designable Aluminum Molecular Rings: Ring Expansion and Ligand Functionalization. Angewandte Chemie - International Edition, 2020, 59, 16735-16740.	13.8	54
139	Liquid-Phase Epitaxial Growth of Azapyrene-Based Chiral Metal–Organic Framework Thin Films for Circularly Polarized Luminescence. ACS Applied Materials & Interfaces, 2019, 11, 31421-31426.	8.0	53
140	A water-stable zeolite-like metal–organic framework for selective separation of organic dyes. RSC Advances, 2014, 4, 1480-1483.	3.6	52
141	Chiral-Induced Ultrathin Covalent Organic Frameworks Nanosheets with Tunable Circularly Polarized Luminescence. Journal of the American Chemical Society, 2022, 144, 7245-7252.	13.7	52
142	Paratactic Assembly of Two Distinct Units into a Unique 3D Architecture. Crystal Growth and Design, 2005, 5, 1313-1315.	3.0	51
143	Comparative Study of Activation Methods on Tuning Gas Sorption Properties of a Metal–Organic Framework with Nanosized Ligands. Inorganic Chemistry, 2012, 51, 11232-11234.	4.0	51
144	Zinc(II)-boron(III)-imidazolate framework (ZBIF) with unusual pentagonal channels prepared from deep eutectic solvent. Dalton Transactions, 2010, 39, 697-699.	3.3	50

#	Article	IF	CITATIONS
145	Homochiral porous metal–organic frameworks containing only achiral building blocks for enantioselective separation. Journal of Materials Chemistry, 2012, 22, 16288.	6.7	50
146	Tuning structural topologies of five photoluminescent Cd(II) coordination polymers through modifying the substitute group of organic ligand. Journal of Solid State Chemistry, 2013, 199, 42-48.	2.9	50
147	Porous <i>ctn</i> â€Type Boron Imidazolate Framework for Gas Storage and Separation. Chemistry - A European Journal, 2013, 19, 11527-11530.	3.3	50
148	Titanium–Oxo Cluster Based Precise Assembly for Multidimensional Materials. Chemistry of Materials, 2017, 29, 2681-2684.	6.7	50
149	Boosting electrocatalytic hydrogen evolution by plasmon-driven hot-electron excitation. Nanoscale, 2018, 10, 2236-2241.	5.6	50
150	Spontaneous asymmetrical crystallization of a three-dimensional diamondoid framework material from achiral precursors. Chemical Communications, 2010, 46, 1449.	4.1	49
151	Facile synthesis of bimetal Au–Ag nanoparticles in a Cu(<scp>i</scp>) boron imidazolate framework with mechanochromic properties. Chemical Communications, 2015, 51, 1353-1355.	4.1	49
152	Optical Resolution of the Water-Soluble Ti ₄ (embonate) ₆ Cages for Enantioselective Recognition of Chiral Drugs. Chemistry of Materials, 2018, 30, 7769-7775.	6.7	49
153	Designable Assembly of Aluminum Molecular Rings for Sequential Confinement of Iodine Molecules. Angewandte Chemie - International Edition, 2021, 60, 21426-21433.	13.8	49
	Neutral and reduced Roussin's red salt ester [Fe ₂ (μ-RS) ₂ (NO) ₄] (R) Tj E	TQq0 0 0	rgBT /Overloc
154	spectroscopic, electrochemical and density functional theoretical investigations. Dalton Transactions, 2009, , 777-786.	3.3	48
155	Zeolitic BIF Crystal Directly Producing Noble-Metal Nanoparticles in Its Pores for Catalysis. Scientific Reports, 2014, 4, 3923.	3.3	48
156	Spontaneous Resolution of Racemic Camphorates in the Formation of Three-Dimensional Metalâ^'Organic Frameworks. Inorganic Chemistry, 2009, 48, 6356-6358.	4.0	47
157	Multifunctional Anionic MOF Material for Dye Enrichment and Selective Sorption of C ₂ Hydrocarbons over Methane via Ag ⁺ -Exchange. Inorganic Chemistry, 2014, 53, 12973-12976.	4.0	47
158	A stable zinc-4-carboxypyrazole framework with high uptake and selectivity of light hydrocarbons. Dalton Transactions, 2015, 44, 2893-2896.	3.3	47
159	Gas Sorption, Second-Order Nonlinear Optics, and Luminescence Properties of a Multifunctional srs-Type Metal–Organic Framework Built by Tris(4-carboxylphenylduryl)amine. Inorganic Chemistry, 2015, 54, 6653-6656.	4.0	47
160	Azole Functionalized Polyoxo-Titanium Clusters with Sunlight-Driven Dye Degradation Applications: Synthesis, Structure, and Photocatalytic Studies. Inorganic Chemistry, 2016, 55, 10294-10301.	4.0	47
161	Syntheses, Structures and Characterisation of Two Cull Polymers with 8-Connected Topologies Based on Highly Connected SBUs. European Journal of Inorganic Chemistry, 2006, 2006, 2253-2258.	2.0	46
162	Visualizing Structural Transformation and Guest Binding in a Flexible Metal–Organic Framework under High Pressure and Room Temperature. ACS Central Science, 2018, 4, 1194-1200.	11.3	46

#	Article	IF	CITATIONS
163	Co (II) Boron Imidazolate Framework with Rigid Auxiliary Linkers for Stable Electrocatalytic Oxygen Evolution Reaction. Advanced Science, 2019, 6, 1801920.	11.2	46
164	Liquid-Phase Epitaxy Effective Encapsulation of Lanthanide Coordination Compounds into MOF Film with Homogeneous and Tunable White-Light Emission. ACS Applied Materials & Interfaces, 2015, 7, 28585-28590.	8.0	45
165	Highly efficient electrocatalysts for overall water splitting: mesoporous CoS/MoS ₂ with hetero-interfaces. Chemical Communications, 2021, 57, 4847-4850.	4.1	45
166	A ligand-conformation driving chiral generation and symmetry-breaking crystallization of a zinc(ii) organoarsonate. Chemical Communications, 2011, 47, 8862.	4.1	44
167	Ionothermal Synthesis of Chiral Metal Phosphite Open Frameworks with In Situ Generated Organic Templates. Inorganic Chemistry, 2013, 52, 5654-5656.	4.0	44
168	Zeolitic Metal–Organic Frameworks Based on Amino Acid. Inorganic Chemistry, 2014, 53, 10027-10029.	4.0	44
169	Structure versatility of coordination polymers constructed from a semirigid ligand and polynuclear metal clusters. CrystEngComm, 2014, 16, 8047-8057.	2.6	44
170	A structure-directing method to prepare semiconductive zeolitic cluster–organic frameworks with Cu ₃ I ₄ building units. Chemical Communications, 2015, 51, 8994-8997.	4.1	44
171	Anionic Metal–Organic Framework for Adsorption and Separation of Light Hydrocarbons. Inorganic Chemistry, 2015, 54, 3093-3095.	4.0	44
172	A boron imidazolate framework with mechanochromic and electrocatalytic properties. Materials Horizons, 2018, 5, 1151-1155.	12.2	44
173	Deliberate design of a neutral heterometallic organic framework containing a record 25-fold interpenetrating diamondoid network. CrystEngComm, 2012, 14, 6359.	2.6	43
174	The photoluminescence and gas sorption properties of three Cd(ii) MOFs based on 1,3,5-benzenetribenzoate with –NH2 or –OH groups. Dalton Transactions, 2014, 43, 4668.	3.3	43
175	Homochiral Metal–Organic Frameworks with Enantiopure Proline Units for the Catalytic Synthesis of β-Lactams. Inorganic Chemistry, 2014, 53, 12199-12204.	4.0	43
176	Two luminescent Cu(i) coordination polymers based on the 1-(4-tetrazolephenyl)imidazole ligand for sensing of nitrobenzene. Inorganic Chemistry Frontiers, 2014, 1, 389.	6.0	43
177	Five porous zinc(<scp>ii</scp>) coordination polymers functionalized with amide groups: cooperative and size-selective catalysis. Journal of Materials Chemistry A, 2015, 3, 20210-20217.	10.3	43
178	Novel Copper(I)â^' and Copper(II)â^'Guanazolate Complexes: Structure, Network Topologies, Photoluminescence, and Magnetic Properties. Crystal Growth and Design, 2008, 8, 3735-3744.	3.0	42
179	Solvent controlled assembly of four Mn(ii)-2,5-thiophenedicarboxylate frameworks with rod-packing architectures and magnetic properties. CrystEngComm, 2013, 15, 6009.	2.6	42
180	Urothermal synthesis of photoluminescent lanthanide–organic frameworks with unusual topologies. CrystEngComm, 2013, 15, 315-323.	2.6	42

#	Article	IF	CITATIONS
181	Structural Transformation and Hysteretic Sorption of Light Hydrocarbons in a Flexible Zn–Pyrazole–Adenine Framework. Chemistry - A European Journal, 2015, 21, 5700-5703.	3.3	41
182	Surface-mounted MOF templated fabrication of homochiral polymer thin film for enantioselective adsorption of drugs. Chemical Communications, 2017, 53, 1470-1473.	4.1	41
183	Induction of Chirality in a Metal–Organic Framework Built from Achiral Precursors. Angewandte Chemie - International Edition, 2021, 60, 3087-3094.	13.8	41
184	In Situ Obtained Cu(II) Compound with Coexistence of Polycatenation and Polythreading. Crystal Growth and Design, 2009, 9, 20-23.	3.0	40
185	New mimic of zeolite: heterometallic organic host framework accommodating inorganic cations. Chemical Communications, 2010, 46, 3182.	4.1	40
186	Synthesis of boron imidazolate frameworks with cobalt clusters for efficient visible-light driven CO ₂ reduction. Journal of Materials Chemistry A, 2019, 7, 17272-17276.	10.3	40
187	Templated synthesis of cobalt subnanoclusters dispersed N/C nanocages from COFs for highly-efficient oxygen reduction reaction. Chemical Engineering Journal, 2020, 401, 126149.	12.7	40
188	Atomically defined Co on two-dimensional TiO2 nanosheet for photocatalytic hydrogen evolution. Chemical Engineering Journal, 2021, 420, 127681.	12.7	40
189	New Coordination Motifs of Melamine Directed by Nâ^'H···X (X = Cl or Br) Hydrogen Bonds. Inorganic Chemistry, 2007, 46, 5838-5840.	4.0	39
190	Serine-Based Homochiral Nanoporous Frameworks for Selective CO ₂ Uptake. Inorganic Chemistry, 2011, 50, 11527-11531.	4.0	39
191	Temperature-Dependent Crystal Self-Assembly, Disassembly, and Reassembly Among Three Cadmium(II) Carboxylate-Phosphinates. Crystal Growth and Design, 2012, 12, 2052-2058.	3.0	39
192	Diverse tetrahedral tetrazolate frameworks with N-rich surface. Chemical Communications, 2016, 52, 5625-5628.	4.1	39
193	Assembly of titanium-oxo cations with copper-halide anions to form supersalt-type cluster-based materials. Chemical Communications, 2017, 53, 3949-3951.	4.1	39
194	Host–Guest Thin Films by Confining Ultrafine Pt/C QDs into Metalâ€Organic Frameworks for Highly Efficient Hydrogen Evolution. Small, 2020, 16, e2005111.	10.0	39
195	Designable Al ₃₂ â€Oxo Clusters with Hydrotalciteâ€like Structures: Snapshots of Boundary Hydrolysis and Optical Limiting. Angewandte Chemie - International Edition, 2021, 60, 4849-4854.	13.8	39
196	Black Titanium-Oxo Clusters with Ultralow Band Gaps and Enhanced Nonlinear Optical Performance. Journal of the American Chemical Society, 2022, 144, 8153-8161.	13.7	39
197	Single- or double-stranded helices-sustained molecular bilayer architecture. CrystEngComm, 2008, 10, 1345.	2.6	38
198	Ring-size controllable metallamacrocycles as building blocks for the construction of microporous metal–organic frameworks. Chemical Communications, 2012, 48, 3653.	4.1	38

#	Article	IF	CITATIONS
199	Chiral assembly of dodecahedral cavities into porous metal–organic frameworks. Chemical Communications, 2012, 48, 9424.	4.1	38
200	Zeolitic Boron Imidazolate Frameworks with 4 onnected Octahedral Metal Centers. Chemistry - A European Journal, 2012, 18, 11876-11879.	3.3	38
201	Microporous Metal–Organic Framework Based on Mixing Nanosized Tris((4-carboxyl)-phenylduryl)amine and 4,4′-Bipyridine Ligands for Gas Storage and Separation. Crystal Growth and Design, 2012, 12, 2468-2471.	3.0	38
202	Tetrahedral Polyoxometalate Nanoclusters with Tetrameric Rare-Earth Cores and Germanotungstate Vertexes. Crystal Growth and Design, 2013, 13, 4368-4377.	3.0	38
203	Achievement of Bulky Homochirality in Zeolitic Imidazolate-Related Frameworks. Inorganic Chemistry, 2015, 54, 11064-11066.	4.0	38
204	CoMo-bimetallic N-doped porous carbon materials embedded with highly dispersed Pt nanoparticles as pH-universal hydrogen evolution reaction electrocatalysts. Nanoscale, 2020, 12, 19804-19813.	5.6	38
205	Threefold Collaborative Stabilization of Ag ₁₄ â€Nanorods by Hydrophobic Ti ₁₆ â€Oxo Clusters and Alkynes: Designable Assembly and Solidâ€State Opticalâ€Limiting Application. Angewandte Chemie - International Edition, 2021, 60, 12949-12954.	13.8	38
206	Co-chelation of a scorpion-shaped carboxylate ligand and phenanthroline lead to a 2-D interpenetratively tubular architecture. CrystEngComm, 2004, 6, 315.	2.6	37
207	A series of three-dimensional lanthanide(iii) coordination polymers of 2,5-dihydroxy-1,4-benzenedicarboxylic acid based on dinuclear lanthanide units. CrystEngComm, 2011, 13, 4981.	2.6	37
208	Interpenetrated Three-Dimensional Copper–lodine Cluster-Based Framework with Enantiopure Porphyrin-like Templates. Inorganic Chemistry, 2016, 55, 1358-1360.	4.0	37
209	Connecting Titanium-Oxo Clusters by Nitrogen Heterocyclic Ligands to Produce Multiple Cluster Series with Photocatalytic H ₂ Evolution Activities. Crystal Growth and Design, 2017, 17, 3592-3595.	3.0	37
210	Selectivity of CO ₂ via pore space partition in zeolitic boron imidazolate frameworks. Chemical Communications, 2016, 52, 3552-3555.	4.1	36
211	Epitaxial encapsulation of homodispersed CeO ₂ in a cobalt–porphyrin network derived thin film for the highly efficient oxygen evolution reaction. Journal of Materials Chemistry A, 2017, 5, 20126-20130.	10.3	36
212	Deep eutectic-solvothermal synthesis of titanium-oxo clusters protected by π-conjugated chromophores. Chemical Communications, 2017, 53, 8078-8080.	4.1	36
213	Liquid Phase Epitaxial Growth and Optical Properties of Photochromic Guest-Encapsulated MOF Thin Film. Crystal Growth and Design, 2016, 16, 5487-5492.	3.0	35
214	Enantiopure anion templated synthesis of a zeolitic metal–organic framework. Chemical Communications, 2016, 52, 1923-1925.	4.1	35
215	Use of aligned triphenylamine-based radicals in a porous framework for promoting photocatalysis. Applied Catalysis B: Environmental, 2018, 221, 664-669.	20.2	35
216	Nanocage-Based Porous Metal–Organic Frameworks Constructed from Icosahedrons and Tetrahedrons for Selective Gas Adsorption. ACS Applied Materials & Interfaces, 2019, 11, 20104-20109.	8.0	35

#	Article	IF	CITATIONS
217	Tetrahedral Geometry Induction of Stable Ag–Ti Nanoclusters by Flexible Trifurcate TiL ₃ Metalloligand. Journal of the American Chemical Society, 2020, 142, 12784-12790.	13.7	35
218	Surface-coordinated metal–organic framework thin films (SURMOFs) for electrocatalytic applications. Nanoscale, 2020, 12, 12712-12730.	5.6	35
219	Homochiral Metal–Organic Framework with Intrinsic Chiral Topology and Helical Channels. Crystal Growth and Design, 2015, 15, 1568-1571.	3.0	34
220	Asymmetric induction in homochiral MOFs: from interweaving double helices to single helices. Chemical Communications, 2015, 51, 16331-16333.	4.1	34
221	Synthesis of homochiral zeolitic metal–organic frameworks with amino acid and tetrazolates for chiral recognition. RSC Advances, 2017, 7, 4872-4875.	3.6	34
222	van der Waals Epitaxial Growth of 2D Metal–Porphyrin Framework Derived Thin Films for Dye‣ensitized Solar Cells. Advanced Materials Interfaces, 2018, 5, 1800985.	3.7	34
223	Tunable chiroptical application by encapsulating achiral lanthanide complexes into chiral MOF thin films. Nano Research, 2022, 15, 1102-1108.	10.4	34
224	Amine-Controlled Assembly of Metalâ^'Sulfite Architecture from 1D Chains to 3D Framework. Inorganic Chemistry, 2007, 46, 6283-6290.	4.0	33
225	Homochiral assembly of polycatenated bilayers with mixing achiral ligands. CrystEngComm, 2012, 14, 789-791.	2.6	33
226	Tetrahedral tetrazolate frameworks for high CO ₂ and H ₂ uptake. Dalton Transactions, 2014, 43, 3210-3214.	3.3	33
227	Homochiral Cluster-Organic Frameworks Constructed from Enantiopure Lactate Derivatives. Crystal Growth and Design, 2015, 15, 4676-4686.	3.0	33
228	Synthesis of an Enantipure Tetrazole-Based Homochiral Cu ^{I,II} -MOF for Enantioselective Separation. Inorganic Chemistry, 2016, 55, 12520-12522.	4.0	33
229	Epitaxial Growth of Highly Transparent Metal–Porphyrin Framework Thin Films for Efficient Bifacial Dye-Sensitized Solar Cells. ACS Applied Materials & Interfaces, 2020, 12, 1078-1083.	8.0	33
230	A twisting chiral â€~dense' 75.9 net, incorporating a helical sub-structure. CrystEngComm, 2005, 7, 177-178.	2.6	32
231	Two Cobalt(II) 5-Aminoisophthalate Complexes and Their Stable Supramolecular Microporous Frameworks. Inorganic Chemistry, 2006, 45, 6276-6281.	4.0	32
232	Cooperative ion-exchange and self-redox process to load catalytic metal nanoparticles into a MOF with Johnson-type cages. Chemical Communications, 2014, 50, 6153.	4.1	32
233	Epitaxial Growth of Oriented Metalloporphyrin Network Thin Film for Improved Selectivity of Volatile Organic Compounds. Small, 2017, 13, 1604035.	10.0	32
234	Helical carbon tubes derived from epitaxial Cu-MOF coating on textile for enhanced supercapacitor performance. Dalton Transactions, 2018, 47, 5558-5563.	3.3	32

#	Article	IF	CITATIONS
235	A novel 3D framework generated by unusual pillared 2D bilayer motifs. New Journal of Chemistry, 2005, 29, 421.	2.8	31
236	Polycatenated 3-connected hydrogen-bonding bilayer stabilized by argentophilic interactions. CrystEngComm, 2007, 9, 636.	2.6	31
237	One-pot synthesis of two isomeric zinc complexes with unusual polycatenation motifs. CrystEngComm, 2007, 9, 390.	2.6	31
238	Protonated 3-amino-1,2,4-triazole templated luminescent lanthanide isophthalates with a rare (3,6)-connected topology. CrystEngComm, 2009, 11, 2734.	2.6	31
239	Syntheses, crystal structures and properties of a series of 3D cadmium coordination polymers with different topologies. Inorganica Chimica Acta, 2010, 363, 1727-1734.	2.4	31
240	Enhancing CO ₂ adsorption enthalpy and selectivity viaamino functionalization of a tetrahedral framework material. CrystEngComm, 2013, 15, 658-661.	2.6	31
241	Acid ontrolled Synthesis of Carboxylateâ€Stabilized Ti ₄₄ â€Oxo Clusters: Scaling up Preparation, Exchangeable Protecting Ligands, and Photophysical Properties. Chemistry - A European Journal, 2019, 25, 10450-10455.	3.3	31
242	A fluorescent Zn–benzotriazole 2D polymer with (6,3) topology. Inorganic Chemistry Communication, 2005, 8, 828-830.	3.9	30
243	Chiral transformations of achiral porous metal–organic frameworks via a stepwise approach. Chemical Communications, 2012, 48, 10419.	4.1	30
244	Controlling State of Breathing of Two Isoreticular Microporous Metal–Organic Frameworks with Triazole Homologues. Chemistry - A European Journal, 2012, 18, 10525-10529.	3.3	30
245	A spin-canted Ni ^{II} ₄ -based metal–organic framework with gas sorption properties and high adsorptive selectivity for light hydrocarbons. Chemical Communications, 2014, 50, 9161.	4.1	30
246	A new cadmium-doped titanium–oxo cluster with stable photocatalytic H ₂ evolution properties. Dalton Transactions, 2016, 45, 4501-4503.	3.3	30
247	Cooperative Self-Assembly of Chiral <scp>l</scp> -Malate and Achiral Succinate in the Formation of a Three-Dimensional Homochiral Framework. Inorganic Chemistry, 2008, 47, 8607-8609.	4.0	29
248	Sizeâ€Dependent Enantioselective Adsorption of Racemic Molecules through Homochiral Metal–Organic Frameworks Embedding Helicity. Chemistry - A European Journal, 2015, 21, 10236-10240.	3.3	29
249	Adsorption of Iodine Based on a Tetrazolate Framework with Microporous Cages and Mesoporous Cages. Inorganic Chemistry, 2016, 55, 13035-13038.	4.0	29
250	Selective Sorption of Light Hydrocarbons on a Family of Metal–Organic Frameworks with Different Imidazolate Pillars. Inorganic Chemistry, 2016, 55, 3928-3932.	4.0	29
251	Synthetic investigation, structural analysis and photocatalytic study of a carboxylate–phosphonate bridged Ti ₁₈ -oxo cluster. Dalton Transactions, 2017, 46, 803-807.	3.3	29
252	Cocrystal of {Ti ₄ } and {Ti ₆ } Clusters with Enhanced Photochemical Properties. Inorganic Chemistry, 2017, 56, 2367-2370.	4.0	28

#	Article	IF	CITATIONS
253	Syntheses of copper–iodine cluster-based frameworks for photocatalytic degradation of methylene blue. CrystEngComm, 2018, 20, 1232-1236.	2.6	28
254	Assembly of high-nuclearity Sn26, Sn34-oxo clusters: solvent strategies and inorganic Sn incorporation. Chemical Science, 2019, 10, 9125-9129.	7.4	28
255	Oriented Assembly of 2D Metal-Pyridylporphyrinic Framework Films for Giant Nonlinear Optical Limiting. Nano Letters, 2021, 21, 10012-10018.	9.1	28
256	Chiral and achiral imidazole-linked tetrahedral zinc phosphonate frameworks with photoluminescent properties. Dalton Transactions, 2014, 43, 285-289.	3.3	27
257	A Series of Homochiral Helical Metal–Organic Frameworks Based on Proline Derivatives. Crystal Growth and Design, 2015, 15, 5901-5909.	3.0	27
258	Synthesis, Structures, and Photocurrent Responses of Polyoxo-Titanium Clusters with Oxime Ligands: From Ti ₄ to Ti ₁₈ . Inorganic Chemistry, 2018, 57, 8850-8856.	4.0	27
259	Subnanometer iron clusters confined in a porous carbon matrix for highly efficient zinc–air batteries. Nanoscale Horizons, 2020, 5, 359-365.	8.0	27
260	Temperatureâ€/Pressureâ€Dependent Selective Separation of CO ₂ or Benzene in a Chiral Metal–Organic Framework Material. ChemSusChem, 2012, 5, 1597-1601.	6.8	26
261	Coordination polymers with free BrÃ,nsted acid sites for selective catalysis. New Journal of Chemistry, 2015, 39, 810-812.	2.8	26
262	Mechanochromic Cu(<scp>i</scp>) boron imidazolate frameworks with low-dimensional structures and reducing function. Inorganic Chemistry Frontiers, 2016, 3, 263-267.	6.0	26
263	Control of Interpenetration and Gas-Sorption Properties of Three Mn(II)-tris((4-carboxyl)phenylduryl)amine Frameworks by Tuning Solvent and Temperature. Crystal Growth and Design, 2017, 17, 290-294.	3.0	26
264	Double defects modified carbon nitride nanosheets with enhanced photocatalytic hydrogen evolution. Physical Chemistry Chemical Physics, 2018, 20, 17471-17476.	2.8	26
265	Alkali/alkaline earth metal and solvents-regulated construction of novel heterometallic coordination polymers based on a semirigid ligand and tetranuclear metal clusters. Inorganica Chimica Acta, 2014, 423, 62-71.	2.4	25
266	Step by Step Bisacrificial Templates Growth of Bimetallic Sulfide QDsâ€Attached MOF Nanosheets for Nonlinear Optical Limiting. Advanced Optical Materials, 2021, 9, 2002072.	7.3	25
267	Surface-coordinated metal-organic framework thin films (SURMOFs): From fabrication to energy applications. EnergyChem, 2021, 3, 100065.	19.1	25
268	A new enantiopure unsaturated dicarboxylate as a 4-connected unit in a flexible homochiral PtS-type framework. Chemical Communications, 2008, , 1756.	4.1	24
269	Host–Guest and Photophysical Behavior of Ti ₈ L ₁₂ Cube with Encapsulated [Ti(H ₂ O) ₆] Species. Chemistry - A European Journal, 2018, 24, 14358-14362.	3.3	24
270	One-Pot and Postsynthetic Phenol-Thermal Synthesis toward Highly Stable Titanium-Oxo Clusters. Inorganic Chemistry, 2019, 58, 13353-13359.	4.0	24

#	Article	IF	CITATIONS
271	Leadâ€Doped Titaniumâ€Oxo Clusters as Molecular Models of Perovskiteâ€Type PbTiO ₃ and Electronâ€Transport Material in Solar Cells. Chemistry - A European Journal, 2020, 26, 6894-6898.	3.3	24
272	Nanosized lanthanide oxide rods in 11O3 hybrid organic–inorganic frameworks involving in situ ligand synthesis. CrystEngComm, 2008, 10, 1088.	2.6	23
273	Metal–organic framework architecture with polyhedron-in-polyhedron and further polyhedral assembly. CrystEngComm, 2013, 15, 1036-1038.	2.6	23
274	Self-Assembly of Metal Boron Imidazolate Cages. Crystal Growth and Design, 2015, 15, 2433-2436.	3.0	23
275	Chiral Chemistry of Homochiral Porous Thin Film with Different Growth Orientations. ACS Applied Materials & Interfaces, 2016, 8, 27332-27338.	8.0	23
276	Construction of unprecedented pillar-layered metal organic frameworks via a dual-ligand strategy for dye degradation. Dalton Transactions, 2018, 47, 4032-4035.	3.3	23
277	Synthesis of Ag-Doped Polyoxotitanium Nanoclusters for Efficient Electrocatalytic CO ₂ Reduction. Inorganic Chemistry, 2020, 59, 11442-11448.	4.0	23
278	Oriented Growth of Inâ€Oxo Chain Based Metalâ€Porphyrin Framework Thin Film for Highâ€Sensitive Photodetector. Advanced Science, 2021, 8, 2100548.	11.2	23
279	Energy Band Alignment and Redoxâ€Active Sites in Metalloporphyrinâ€Spaced Metal atechol Frameworks for Enhanced CO ₂ Photoreduction. Angewandte Chemie - International Edition, 2022, 61, .	13.8	23
280	Host–Guest Pore Space Partition in a Boron Imidazolate Framework for Ethylene Separation. Chemistry of Materials, 2022, 34, 307-313.	6.7	23
281	A rare twofold interpenetrated cds topology in a Zn-organic polymer [Zn2(BDC)(BPP)Cl2]n. Inorganic Chemistry Communication, 2006, 9, 449-451.	3.9	22
282	Novel (3,6)-connected network and (4,6)-connected framework in two copper(II) and cadmium(II) complexes of flexible (2S,3S,4R,5R)-tetrahydrofurantetracarboxylic acid: synthesis, structure, thermostability, and luminescence studies. CrystEngComm, 2009, 11, 1934.	2.6	22
283	Canted antiferromagnetic behaviours in isostructural Co(ii) and Ni(ii) frameworks with helical lvt topology. CrystEngComm, 2010, 12, 2938.	2.6	22
284	Flexible Porous Zinc–Pyrazole–Adenine Framework for Hysteretic Sorption of Light Hydrocarbons. Crystal Growth and Design, 2015, 15, 1210-1213.	3.0	22
285	Zeolitic Tetrazolate–Imidazolate Frameworks with SOD Topology for Room Temperature Fixation of CO ₂ to Cyclic Carbonates. Crystal Growth and Design, 2020, 20, 2866-2870.	3.0	22
286	Temperature-Controlled Syntheses of Substituted 1,2,4-Triazolelead(II) Complexes: Active Lone Pair and Nâ^'H···X (X = Cl, Br, I) Hydrogen Bonds. Inorganic Chemistry, 2009, 48, 9992-9994.	4.0	21
287	Formation of Aminoxy and Oxo Complexes from the Reaction of Nb(NMe ₂) ₅ with O ₂ and the Crystal Structure of Nb(NEt ₂) ₅ . Inorganic Chemistry, 2010, 49, 4017-4022.	4.0	21
288	Structure-dependent mechanochromism of two Ag(<scp>i</scp>) imidazolate chains. CrystEngComm, 2016, 18, 218-221.	2.6	21

#	Article	IF	CITATIONS
289	Facile Synthesis of Metal-Loaded Porous Carbon Thin Films via Carbonization of Surface-Mounted Metal–Organic Frameworks. Inorganic Chemistry, 2017, 56, 3526-3531.	4.0	21
290	Synthesis and photocatalytic H2 evolution properties of four titanium-oxo-clusters based on a cyclohex-3-ene-1-carboxylate ligand. Dalton Transactions, 2017, 46, 10630-10634.	3.3	21
291	Ti ₄ (embonate) ₆ Cage-Ligand Strategy on the Construction of Metal–Organic Frameworks with High Stability and Gas Sorption Properties. Inorganic Chemistry, 2020, 59, 964-967.	4.0	21
292	Experimental and Theoretical Studies on Effects of Structural Modification of Tin Nanoclusters for Third-Order Nonlinear Optical Properties. Inorganic Chemistry, 2021, 60, 1885-1892.	4.0	21
293	Three Copper(II) Coordination Polymers Constructed by Both Rigid and Flexible Ligands. Zeitschrift Fur Anorganische Und Allgemeine Chemie, 2005, 631, 3053-3057.	1.2	20
294	Homochiral moganite-type metal–organic framework based on unusual (Ag2Cl)n skeletons. CrystEngComm, 2008, 10, 655.	2.6	20
295	A microporous indium–organic framework with high capacity and selectivity for CO2 or or or organosulfurs. Dalton Transactions, 2012, 41, 2873.	3.3	20
296	Interpreted Recognition Process: A Highly Sensitive and Selective Luminescence Chemosensor. Chemistry - A European Journal, 2015, 21, 11767-11772.	3.3	20
297	Synthesis of metal-adeninate frameworks with high separation capacity on C2/C1 hydrocarbons. Journal of Solid State Chemistry, 2016, 238, 241-245.	2.9	20
298	Waterâ€ 6 table Homochiral Cluster Organic Frameworks Built by Two Kinds of Large Tetrahedral Cluster Units. Chemistry - A European Journal, 2016, 22, 2611-2615.	3.3	20
299	Ligand dependent assembly of trinuclear titanium-oxo units into coordination tetrahedra and capsules. Dalton Transactions, 2018, 47, 663-665.	3.3	20
300	N-Heterocyclic Carbene as a Surface Platform for Assembly of Homochiral Metal–Organic Framework Thin Films in Chiral Sensing. ACS Applied Materials & Interfaces, 2020, 12, 38357-38364.	8.0	20
301	2D Boron Imidazolate Framework Nanosheets with Electrocatalytic Applications for Oxygen Evolution and Carbon Dioxide Reduction Reaction. Small, 2020, 16, e1907669.	10.0	20
302	Guest selectivity of a porous tetrahedral imidazolate framework material during self-assembly. Journal of Materials Chemistry, 2012, 22, 19732.	6.7	19
303	Organic Cation Templated Synthesis of Three Zinc–2,5-Thiophenedicarboxylate Frameworks for Selective Gas Sorption. Crystal Growth and Design, 2014, 14, 3493-3498.	3.0	19
304	Construction of Cluster Organic Frameworks with <i>bnn</i> Hexagonal BN Topologies. Chemistry - A European Journal, 2015, 21, 15511-15515.	3.3	19
305	Ti ₄ (embonate) ₆ Based Cage-Cluster Construction in a Stable Metal–Organic Framework for Gas Sorption and Separation. Crystal Growth and Design, 2020, 20, 29-32.	3.0	19
306	Syntheses and structures of two novel Ag(I) complexes: [I¼3-2-(4-pyridyl)ethanesulfonato-N,O,Oâ€2]-aqua-silver(I) and melamine-[2-(4-pyridyl)ethanesulfonato-N]-silver(I). Journal of Molecular Structure, 2004, 697, 185-189.	3.6	18

#	Article	IF	CITATIONS
307	A luminescent Cu(I) complex ligated by 1,3-bis(4-pyridyl)trisulfane generated in situ by the coupling of pyridine-4-thiol. Inorganic Chemistry Communication, 2008, 11, 164-166.	3.9	18
308	Ag(I)-Mediated In situ Dehydrogenative Coupling of 3-Amino-1,2,4-triazole into 3,3â€2-Azobis(1,2,4-triazole) in Cd(II) Coordination Polymers. Inorganic Chemistry, 2009, 48, 10859-10861.	4.0	18
309	Configuration determination of flexible tetracarboxylate ligands in two supramolecular structures. CrystEngComm, 2009, 11, 1201.	2.6	18
310	Synthesis of Metal–Organic Zeolites with Homochirality and High Porosity for Enantioselective Separation. Inorganic Chemistry, 2016, 55, 6355-6357.	4.0	18
311	Particular Handedness Excess through Symmetry-Breaking Crystallization of a 3D Cobalt Phosphonate. Inorganic Chemistry, 2016, 55, 537-539.	4.0	18
312	Insight into Fe(Salen) Encapsulated Co-Porphyrin Framework Derived Thin Film for Efficient Oxygen Evolution Reaction. Crystal Growth and Design, 2018, 18, 7150-7157.	3.0	18
313	HZIF-based hybrids for electrochemical energy applications. Nanoscale, 2019, 11, 15763-15769.	5.6	18
314	Engineering nanointerface of molybdenum-based heterostructures to boost the electrocatalytic hydrogen evolution reaction. Journal of Energy Chemistry, 2021, 58, 370-376.	12.9	18
315	A new polar supramolecular 3D framework [Zn(pyz)(H2O)4]pht. Journal of Molecular Structure, 2005, 750, 39-43.	3.6	17
316	Organic templates promoted photocatalytic and photoluminescent properties between two coordination polymers. CrystEngComm, 2013, 15, 10423.	2.6	17
317	A Rational Strategy To Construct a Neutral Boron Imidazolate Framework with Encapsulated Small-Size Au–Pd Nanoparticles for Catalysis. Inorganic Chemistry, 2015, 54, 6069-6071.	4.0	17
318	Zeolitic Tetrazolate-Imidazolate Frameworks with High Chemical Stability for Selective Separation of Small Hydrocarbons. Crystal Growth and Design, 2016, 16, 3063-3066.	3.0	17
319	Encapsulation of Ln ^{III} ions/Ag nanoparticles within Cd(<scp>ii</scp>) boron imidazolate frameworks for tuning luminescence emission. Chemical Communications, 2016, 52, 8577-8580.	4.1	17
320	Structures and photophysical performances of (fluoro)salicylate stabilized polyoxo-titanium clusters. CrystEngComm, 2018, 20, 5964-5968.	2.6	17
321	Hybrid Zeolitic Imidazolate Frameworks for Promoting Electrocatalytic Oxygen Evolution via a Dual-Site Relay Mechanism. Inorganic Chemistry, 2021, 60, 3074-3081.	4.0	17
322	Stepwise assembly and reversible structural transformation of ligated titanium coated bismuth-oxo cores: shell morphology engineering for enhanced chemical fixation of CO ₂ . Chemical Science, 2022, 13, 3395-3401.	7.4	17
323	Syntheses and Crystal Structures of Two Metal Succinates Modified by Bipyridines. Zeitschrift Fur Anorganische Und Allgemeine Chemie, 2004, 630, 2731-2735.	1.2	16
324	Syntheses, structures and photoluminescent properties of 1D, 2D, 3D silver (I) coordination polymers with flexible long-chain dinitriles and tetranitriles. Polyhedron, 2004, 23, 2209-2215.	2.2	16

#	Article	IF	CITATIONS
325	Controlled generation of acentric and homochiral coordination compounds from a versatile asymmetric ligand 4-(1H-1,2,4-triazol-3-yl)-4H-1,2,4-triazole. Chemical Communications, 2008, , 4159.	4.1	16
326	Visible Concentration-Sensitive Structural Transformation. Crystal Growth and Design, 2010, 10, 1464-1467.	3.0	16
327	The first anionic four-connected boron imidazolate framework. Dalton Transactions, 2010, 39, 2487.	3.3	16
328	Multiarylpolycarboxylate-Mediated Hybrid Cobalt Phosphate Frameworks with Supramolecular Zeolitic Topology and Unusual I2O2 Connectivity. Inorganic Chemistry, 2015, 54, 1209-1211.	4.0	16
329	High and selective sorption of C2 hydrocarbons in heterometal–organic frameworks built from tetrahedral units. RSC Advances, 2015, 5, 7794-7797.	3.6	16
330	Dicarboxylate Ligands Oriented Assembly of {Ti ₃ (μ ₃ -O)} Units: From Dimer to Coordination Triangles and Rectangles. Inorganic Chemistry, 2018, 57, 5642-5647.	4.0	16
331	Synthesis of homochiral zeolitic imidazolate frameworks <i>via</i> solvent-assisted linker exchange for enantioselective sensing and separation. CrystEngComm, 2018, 20, 5925-5928.	2.6	16
332	Stabilizing γ-Alkyltin–Oxo Keggin Ions by Borate Functionalization. Inorganic Chemistry, 2019, 58, 4534-4539.	4.0	16
333	Synthesis, structure, and fluorescence of two cadmium(II)-citrate coordination polymers with different coordination architectures. Journal of Molecular Structure, 2005, 740, 223-227.	3.6	15
334	Rare 4.82 net in a fluorescent Cd-organic framework. Inorganic Chemistry Communication, 2005, 8, 722-724.	3.9	15
335	Assembly between various molecular-building-blocks for network diversity of zinc–1,3,5-benzenetricarboxylate frameworks. CrystEngComm, 2012, 14, 8684.	2.6	15
336	Temperature-dependent urothermal synthesis of two distinct La(III)-naphthalenedicarboxylate frameworks. Inorganic Chemistry Communication, 2013, 29, 148-150.	3.9	15
337	Targeted design of a cubic boron imidazolate cage with sensing and reducing functions. Dalton Transactions, 2015, 44, 9367-9369.	3.3	15
338	Insight into the epitaxial encapsulation of Pd catalysts in an oriented metalloporphyrin network thin film for tandem catalysis. Nanoscale, 2017, 9, 7734-7738.	5.6	15
339	Synthesis, structure and proton conductivity of a metal–organic framework with rich hydrogen-bonds between the layers. Inorganic Chemistry Communication, 2017, 79, 37-40.	3.9	15
340	Electrooxidation of Pd–Cu NP loaded porous carbon derived from a Cu-MOF. RSC Advances, 2018, 8, 1803-1807.	3.6	15
341	A wide pH-range stable crystalline framework based on the largest tin-oxysulfide cluster [Sn20O10S34]. Chemical Communications, 2019, 55, 11083-11086.	4.1	15
342	Mixed Short and Long Ligands toward the Construction of Metal–Organic Frameworks with Large Pore Openings. Crystal Growth and Design, 2019, 19, 3120-3123.	3.0	15

#	Article	IF	CITATIONS
343	Co ₉ S ₈ integrated into nitrogen/sulfur dual-doped carbon nanofibers as an efficient oxygen bifunctional electrocatalyst for Zn–air batteries. Sustainable Energy and Fuels, 2020, 4, 1093-1098.	4.9	15
344	Composite of CsPbBr ₃ with Boron Imidazolate Frameworks as an Efficient Visible-Light Photocatalyst for CO ₂ Reduction. ACS Applied Energy Materials, 2022, 5, 1175-1182.	5.1	15
345	Magnetic investigation of two helical frameworks derived from mixed ligands. Inorganica Chimica Acta, 2007, 360, 3525-3532.	2.4	14
346	Hydrogen-bonded boron imidazolate frameworks. Dalton Transactions, 2010, 39, 1702-1704.	3.3	14
347	Optimization of Reaction Conditions towards Multiple Types of Framework Isomers and Periodicâ€Increased Porosity: Luminescence Properties and Selective CO ₂ Adsorption over N ₂ . ChemPhysChem, 2013, 14, 3594-3599.	2.1	14
348	Catenation of Homochiral Metal–Organic Nanocages or Nanotubes. Inorganic Chemistry, 2016, 55, 5095-5097.	4.0	14
349	Structural Design of Zeolitic Cluster Organic Frameworks from Hexamethylentetramine and Copper-Halide Clusters. Crystal Growth and Design, 2016, 16, 7139-7144.	3.0	14
350	Construction of molecular rectangles with titanium–oxo clusters and rigid aromatic carboxylate ligands. Dalton Transactions, 2017, 46, 16000-16003.	3.3	14
351	Synthesis of Homochiral Zeolitic Tetrazolate Frameworks Based on Enantiopure Porphyrin-like Subunits. Crystal Growth and Design, 2017, 17, 5393-5397.	3.0	14
352	Fast Synthesis of Hybrid Zeolitic Imidazolate Frameworks (HZIFs) with Exceptional Acid–Base Stability from ZIF-8 Precursors. Crystal Growth and Design, 2019, 19, 3430-3434.	3.0	14
353	Self-Assembly of a Ti ₄ (embonate) ₆ Cage toward Silver. Inorganic Chemistry, 2020, 59, 14861-14865.	4.0	14
354	Synthesis of Supramolecular Boron Imidazolate Frameworks for CO ₂ Photoreduction. Inorganic Chemistry, 2020, 59, 17851-17855.	4.0	14
355	Designable Aluminum Molecular Rings: Ring Expansion and Ligand Functionalization. Angewandte Chemie, 2020, 132, 16878-16883.	2.0	14
356	Design of Hybrid Zeolitic Imidazolate Frameworkâ€Derived Material with C–Mo–S Triatomic Coordination for Electrochemical Oxygen Reduction. Small, 2021, 17, e2003256.	10.0	14
357	Epitaxial growth of prussian blue analogue derived NiFeP thin film for efficient electrocatalytic hydrogen evolution reaction. Journal of Solid State Chemistry, 2021, 293, 121779.	2.9	14
358	Twofold parallely interpenetrated 2D polymers of d10 zinc and cadmium based on mixed nicotinate/isonicotinate ligands. Journal of Molecular Structure, 2007, 827, 126-129.	3.6	13
359	A microporous nickel–organic framework with an unusual 10-connected bct net and high capacity for CO2, H2 and hydrocarbons. CrystEngComm, 2013, 15, 9499.	2.6	13
360	Encapsulation of an Interpenetrated Diamondoid Inorganic Building Block in a Metal–Organic Framework. Chemistry - A European Journal, 2015, 21, 4931-4934.	3.3	13

#	Article	IF	CITATIONS
361	A couple of Co(II) enantiomers constructed from semirigid lactic acid derivatives. Inorganic Chemistry Communication, 2016, 73, 115-118.	3.9	13
362	Ligand-directed assembly engineering of trapezoidal {Ti ₅ } building blocks stabilized by dimethylglyoxime. Dalton Transactions, 2019, 48, 9916-9919.	3.3	13
363	Amino-Polyalcohol-Solvothermal Synthesis of Titanium-Oxo Clusters: From Ti ₆ to Ti ₁₉ with Structural Diversity. Inorganic Chemistry, 2019, 58, 7267-7273.	4.0	13
364	Pyrazole-thermal synthesis: a new approach towards N-rich titanium-oxo clusters with photochromic behaviors. Dalton Transactions, 2019, 48, 8049-8052.	3.3	13
365	Synthesis of Anionic Metal–Organic Zeolites for Selective Gas Adsorption and Ion Exchange. Inorganic Chemistry, 2019, 58, 4076-4079.	4.0	13
366	Chiral induction in a pcu -derived network from achiral precursors. Chemical Communications, 2019, 55, 4611-4614.	4.1	13
367	A supersalt-type copper(<scp>i</scp>)-thiolate cluster with applications for mechano/thermochromism and the oxygen evolution reaction. Chemical Communications, 2020, 56, 3967-3970.	4.1	13
368	Investigation on the variation regularity of the characteristic droplet diameters in the swirling flow field. Chemical Engineering Science, 2021, 229, 116153.	3.8	13
369	Tin Metal Cluster Compounds as New Third-Order Nonlinear Optical Materials by Computational Study. Journal of Physical Chemistry Letters, 2021, 12, 7537-7544.	4.6	13
370	Novel Third-Order Nonlinear Optical Materials with Craig-Möbius Aromaticity. Journal of Physical Chemistry Letters, 2021, 12, 11784-11789.	4.6	13
371	Optimizing Photodetectors in Two-Dimensional Metal-Metalloporphyrinic Framework Thin Films. ACS Applied Materials & Interfaces, 2022, 14, 33548-33554.	8.0	13
372	Doubly interpenetrated hms-type metal organic framework formed by perfect face-to-face π…π stacking interactions. Inorganic Chemistry Communication, 2010, 13, 1429-1431.	3.9	12
373	Hydrogen-bond-directed self-assembly of a novel 2D→3D polythreading with finite components based on rigid ligand. Journal of Molecular Structure, 2011, 994, 1-5.	3.6	12
374	Redox Reaction Induced Structural Transformation among Three Copper Coordination Polymers. Crystal Growth and Design, 2012, 12, 5164-5168.	3.0	12
375	Digital Controlled Luminescent Emission via Patterned Deposition of Lanthanide Coordination Compounds. ACS Applied Materials & amp; Interfaces, 2014, 6, 12594-12599.	8.0	12
376	Halogen dependent symmetry change in two series of wheel cluster organic frameworks built from La ₁₈ tertiary building units. Chemical Communications, 2016, 52, 1455-1457.	4.1	12
377	Synthesis of a Homochiral Metal–Organic Zeolite for Enantioselective Sensing and Separation. Crystal Growth and Design, 2020, 20, 5644-5647.	3.0	12
378	Two Isostructural Titanium Metal–Organic Frameworks for Light Hydrocarbon Separation. Inorganic Chemistry, 2021, 60, 13955-13959.	4.0	12

#	Article	IF	CITATIONS
379	Assembly of Four Kinds of Cages into Porous Metal–Organic Framework for Selective Sorption of Light Hydrocarbons. Crystal Growth and Design, 2014, 14, 6467-6471.	3.0	11
380	Integration of a semi-rigid proline ligand and 4,4′-bipyridine in the synthesis of homochiral metal–organic frameworks with helices. Dalton Transactions, 2015, 44, 11052-11056.	3.3	11
381	A zeolitic Cd(II) boron imidazolate framework with sensing and catalytic properties. Journal of Solid State Chemistry, 2015, 231, 185-189.	2.9	11
382	A pair of novel 4-connected homochiral coordination polymers based on proline-tetrazole ligand. Inorganic Chemistry Communication, 2016, 67, 44-46.	3.9	11
383	Synthesis of zeolite-like metal–organic frameworks via a dual-ligand strategy. CrystEngComm, 2017, 19, 2549-2552.	2.6	11
384	Embonic Acid Functionalized Niobium Complexes with Selective Dye Sorption Properties. Inorganic Chemistry, 2018, 57, 4226-4229.	4.0	11
385	A core–shell type alkyl-Sn-oxo cluster of {Sn ₁₄ As ₁₆ } bridged by 4-aminophenylarsonate ligands and incorporated with a {Na ₆ } cluster. Chemical Communications, 2020, 56, 1433-1435.	4.1	11
386	Surface chiroselective assembly of enantiopure crystalline porous films containing bichiral building blocks. Chemical Science, 2021, 12, 12346-12352.	7.4	11
387	Molecular bixbyite-like In ₁₂ -oxo clusters with tunable functionalization sites for lithography patterning applications. Chemical Science, 2021, 12, 14414-14419.	7.4	11
388	Chiral induction in boron imidazolate frameworks: the construction of cage-based absolute helices. Chemical Communications, 2021, 57, 5020-5023.	4.1	11
389	Phosphorescent Calcium-Based Metal–Organic Framework with Second-Scale Long Afterglow. Inorganic Chemistry, 2021, 60, 10075-10078.	4.0	11
390	Synergistic Lewis acid and Pd active sites of metal–organic frameworks for highly efficient carbonylation of methyl nitrite to dimethyl carbonate. Inorganic Chemistry Frontiers, 2022, 9, 2379-2388.	6.0	11
391	Urothermal synthesis and distinct thermal behavior of isostructural transition metal-based MIL-53 analogs. Solid State Sciences, 2012, 14, 1263-1266.	3.2	10
392	Syntheses, crystal structures and fluorescent properties of three metal- tris(4′-carboxybiphenyl)amine frameworks. Journal of Solid State Chemistry, 2017, 255, 200-205.	2.9	10
393	Syntheses, crystal structures and fluorescent properties of two metal-organic frameworks based on pamoic acid. Journal of Solid State Chemistry, 2019, 270, 335-338.	2.9	10
394	Construction of Metal–Organic Frameworks with Various Zinc-Tetrazolate Nanotubes. Crystal Growth and Design, 2021, 21, 28-32.	3.0	10
395	Polyoxo-titanium clusters promoted photocatalytic H2 evolution activity in a NiS modified CdS/MIL-101 system. International Journal of Hydrogen Energy, 2021, 46, 6369-6379.	7.1	10
396	Aluminium nanorings: configuration deformation and structural transformation. Chemical Communications, 2021, 57, 2085-2088.	4.1	10

#	Article	IF	CITATIONS
397	Synthesis of a Boron–Imidazolate Framework Nanosheet with Dimer Copper Units for CO 2 Electroreduction to Ethylene. Angewandte Chemie, 2021, 133, 16823-16828.	2.0	10
398	Design and synthesis of zeolitic tetrazolate-imidazolate frameworks. Materials Today Advances, 2021, 10, 100145.	5.2	10
399	Protection of Ag Clusters by Metalâ€Oxo Modules. Chemistry - A European Journal, 2021, 27, 15563-15570.	3.3	10
400	Sn ₆ and Na ₄ Oxo Clusters Based Non-centrosymmetric Framework for Solution Iodine Absorption and Second Harmonic Generation Response. Inorganic Chemistry, 2021, 60, 1985-1990.	4.0	10
401	Syntheses and Characterizations of Two Novel Silver(I) Complexes Constructed by Oxydipropionitrile Ligand. Crystal Growth and Design, 2005, 5, 73-75.	3.0	9
402	Urothermal synthesis of a photoluminescent zinc coordination polymer. Inorganic Chemistry Communication, 2011, 14, 355-357.	3.9	9
403	Synthesis and gas sorption properties of a homochiral metal–organic framework with octahedral cages. CrystEngComm, 2015, 17, 6107-6109.	2.6	9
404	Unique microporous NbO-type Coll/Znll MOFs from double helical chains: Sorption and luminescent properties. Journal of Solid State Chemistry, 2016, 238, 170-174.	2.9	9
405	Improving the photocatalytic H2 evolution activities of TiO2 by modulating the stabilizing ligands of the nanoscale Ti8O8-cluster precursors. International Journal of Hydrogen Energy, 2017, 42, 24737-24743.	7.1	9
406	Polycatenation tuned microporosity of two metal–tris(4′-carboxybiphenyl)amine frameworks with multilayer structures. Dalton Transactions, 2017, 46, 13352-13355.	3.3	9
407	Synthesis of zeolitic tetrazolate-imidazolate frameworks (ZTIFs) in ethylene glycol. Inorganic Chemistry Frontiers, 2018, 5, 675-678.	6.0	9
408	Stepwise Coordination Assembly Approach toward Aluminum-Lanthanide-based Compounds. Inorganic Chemistry, 2020, 59, 13760-13766.	4.0	9
409	Supramolecular Co-assembly of the Ti ₈ L ₁₂ Cube with [Ti(DMF) ₆] Species and Ti ₁₂ -Oxo Cluster. Inorganic Chemistry, 2020, 59, 8291-8297.	4.0	9
410	Synergistic ligand effect for the construction of titanium–oxo clusters with planar chirality and high solution stability. Dalton Transactions, 2020, 49, 4030-4033.	3.3	9
411	Combining a Titanium–Organic Cage and a Hydrogenâ€Bonded Organic Cage for Highly Effective Thirdâ€Order Nonlinear Optics. Angewandte Chemie, 2021, 133, 2956-2959.	2.0	9
412	Single-Crystal Syntheses and Properties of Indium–Organic Frameworks Based on 1,1′-Ferrocenedicarboxylic Acid. Inorganic Chemistry, 2021, 60, 239-245.	4.0	9
413	Aluminum molecular rings bearing amino-polyalcohol for iodine capture. Inorganic Chemistry Frontiers, 2022, 9, 592-598.	6.0	9
414	Structural diversity and distinct photoluminescent properties of two new lanthanide-copper (I) frameworks based on mixed isonicontinate/oxalate ligands. Inorganic Chemistry Communication, 2010, 13, 938-940.	3.9	8

#	Article	IF	CITATIONS
415	Rare 5-connected BN topology in homochiral Cd(II) camphorate with 2-(4-pyridyl)benzimidazole. Inorganic Chemistry Communication, 2011, 14, 228-230.	3.9	8
416	Rational design of metal boron imidazolate cages to frameworks. Inorganica Chimica Acta, 2017, 460, 89-92.	2.4	8
417	Coordination Assembly of the Waterâ€Soluble Ti 4 (embonate) 6 Cages with Mn 2+ Ions. Israel Journal of Chemistry, 2019, 59, 233-236.	2.3	8
418	A green separation process of Ag <i>via</i> a Ti ₄ (embonate) ₆ cage. Dalton Transactions, 2020, 49, 17194-17199.	3.3	8
419	Synthesis and photocatalytic activities of two homochiral metal–organic frameworks with cages and hydrogen bonding helices. CrystEngComm, 2020, 22, 4206-4209.	2.6	8
420	Tin-oxychalcogenide supertetrahedral clusters maintained in a MTN zeolite-analog arrangement by coulombic interactions. Chemical Communications, 2020, 56, 8388-8391.	4.1	8
421	A metal-porphyrinic framework film as an efficient optical limiting layer in an electro-optical switchable device. Chemical Communications, 2021, 57, 10166-10169.	4.1	8
422	An Anionic MOF for Separation of Organic Dyes via Cationic-Exchange and Size-Exclusion. Acta Chimica Sinica, 2014, 72, 1228.	1.4	8
423	Tunable third-order nonlinear optical effect <i>via</i> modifying Ti ₄ (embonate) ₆ cage-based ionic pairs. Inorganic Chemistry Frontiers, 2022, 9, 1984-1991.	6.0	8
424	An inorganic–organic hybrid zinc phosphite framework with unusual topology. Inorganic Chemistry Communication, 2013, 30, 136-138.	3.9	7
425	A highly stable face-extended diamondoid cluster–organic framework incorporating infinite inorganic guests. Chemical Communications, 2015, 51, 17174-17177.	4.1	7
426	Sn ₁₃ –Oxo Clusters with an Open Hollow Structural Motif and Decorated by Different Functional Ligands. Inorganic Chemistry, 2019, 58, 15692-15695.	4.0	7
427	Heterometallic Ag ₂ Ti ₁₀ and Ag ₄ Ti ₈ -oxo clusters with different silver doping models: synthesis, structure, and theoretical studies. Dalton Transactions, 2020, 49, 11005-11009.	3.3	7
428	Optical Resolution Studies on Ti/Zr-Based Tetrahedral Cages. Crystal Growth and Design, 2020, 20, 6316-6320.	3.0	7
429	Assembly and packing models of [Ti6Co12] ring based on the titanium-capped cobalt clathrochelates. Chinese Chemical Letters, 2021, 32, 923-925.	9.0	7
430	A Cu(<scp>i</scp>) based boron imidazolate framework for visible light driven CO ₂ reduction. Dalton Transactions, 2021, 50, 490-493.	3.3	7
431	A hybrid zeolitic imidazolate framework-derived ZnO/ZnMoO ₄ heterostructure for electrochemical hydrogen production. Dalton Transactions, 2021, 50, 11365-11369.	3.3	7
432	Coordination Assembly of Tetrahedral Zr ₄ (embonate) ₆ Cages with Eu ³⁺ lons. Inorganic Chemistry, 2021, 60, 18178-18184.	4.0	7

#	Article	IF	CITATIONS
433	Acid–base resistant ligand-modified molybdenum–sulfur clusters with enhanced photocatalytic activity towards hydrogen evolution. Journal of Materials Chemistry A, 2022, 10, 7138-7145.	10.3	7
434	A luminescent neutral cadmium(ii)–boron(iii)–imidazolate framework with sql net. CrystEngComm, 2014, 16, 2889.	2.6	6
435	Tuning Photoluminescence Emission of a Cadmium–Organic Framework by Excitation. ChemPlusChem, 2014, 79, 1080-1082.	2.8	6
436	An anionic Cd(ii) boron imidazolate framework with reversible structural transformation and biomolecular sensing properties. Dalton Transactions, 2017, 46, 10202-10204.	3.3	6
437	Wheelâ€5hape Heterometallic Ti ₁₀ M ₂ â€oxo Clusters (M = Ni, Co) with Effective Visible Light Absorption. Chinese Journal of Chemistry, 2019, 37, 233-236.	4.9	6
438	Synthesis and Structure of a Series of Ti ₆ â€oxo Clusters Functionalized by <i>in situ</i> Esterified Dicarboxylate Ligands. Chinese Journal of Chemistry, 2021, 39, 1259-1264.	4.9	6
439	Synthesis, Structures, and Fluorescence Properties of Dimeric Aluminum Oxo Clusters. Inorganic Chemistry, 2021, 60, 7089-7093.	4.0	6
440	Phenol-triggered supramolecular transformation of titanium–oxo cluster based coordination capsules. Chinese Chemical Letters, 2021, 32, 2415-2418.	9.0	6
441	Macrocyclic Inorganic Tin ontaining Oxo Clusters: Heterometallic Strategy for Configuration and Catalytic Activity Modulation. Chemistry - A European Journal, 2021, 27, 16117-16120.	3.3	6
442	Syntheses of new zeolitic imidazolate frameworks in dimethyl sulfoxide. Inorganic Chemistry Frontiers, 2022, 9, 2011-2015.	6.0	6
443	Facile Synthesis of a Long Afterglow Calcium–Organic Framework in Water. ACS Omega, 2022, 7, 22015-22019.	3.5	6
444	Divergent Access to Polycyclic <i>N</i> -Heterocyclic Compounds through Büchner-Type Dearomatization Enabled Cycloisomerization of Diynamides under Gold Catalysis. Organic Letters, 2022, 24, 4298-4303.	4.6	6
445	Synthesis of borocarbonitride from a multifunctional Cu(<scp>i</scp>) boron imidazolate framework. Dalton Transactions, 2016, 45, 5223-5228.	3.3	5
446	p-Arsanilic acid stabilizing titanium-oxo clusters with various core structures and light absorption behaviours. Inorganic Chemistry Communication, 2017, 86, 14-17.	3.9	5
447	Tuning a layer to a three-dimensional cobalt-tris(4′-carboxybiphenyl)amine framework by introducing potassium ions. Inorganic Chemistry Communication, 2018, 90, 65-68.	3.9	5
448	Synthesis, structure and luminescent of Ag based homochiral metal tetrazolate coordination polymers. Inorganic Chemistry Communication, 2018, 89, 41-45.	3.9	5
449	Adjustment of the performance and stability of isostructural zeolitic tetrazolate-imidazolate frameworks. Dalton Transactions, 2020, 49, 4690-4693.	3.3	5
450	Unraveling the condensation reactions of heterometallic {BiNb4} moieties into hybrid BixNby-oxo clusters with mass spectrometry. Science China Chemistry, 2021, 64, 413-418.	8.2	5

#	Article	IF	CITATIONS
451	Odd-membered cyclic hetero-polyoxotitanate nanoclusters with high stability and photocatalytic H2 evolution activity. Chinese Journal of Catalysis, 2021, 42, 1332-1337.	14.0	5
452	Induction of Chirality in Boron Imidazolate Frameworks: The Structure-Directing Effects of Substituents. Inorganic Chemistry, 2022, 61, 6861-6868.	4.0	5
453	Synthesis and photoluminescent properties of four homochiral supramolecular compounds with butterfly-like chains. Inorganic Chemistry Communication, 2014, 46, 219-222.	3.9	4
454	A pair of novel Cd(II) enantiomers based on lactate derivatives: Synthesis, crystal structures and properties. Journal of Solid State Chemistry, 2016, 241, 105-109.	2.9	4
455	One unique neutral boron imidazolate framework with fluorescent property. Inorganic Chemistry Communication, 2018, 95, 130-133.	3.9	4
456	Water-stable Zeolitic Tetrazolate-Imidazolate Frameworks (ZTIFs) with GIS topology. Inorganic Chemistry Communication, 2019, 105, 59-62.	3.9	4
457	Construction of Titanium-Based Metal–Organic Frameworks Based on the Ti/Cu Heteronuclear Cluster. Inorganic Chemistry, 2021, 60, 24-27.	4.0	4
458	Functional ligand directed assembly and electronic structure of Sn ₁₈ -oxo wheel nanoclusters. Chemical Communications, 2021, 57, 5159-5162.	4.1	4
459	Syntheses and Structural Studies of a Series of Ti4(embonate)6-based Complexes. Acta Chimica Sinica, 2020, 78, 1411.	1.4	4
460	Triethanolamine stabilized non-alkyl Sn ₄ Cd ₄ and alkyl Sn ₂ Cd ₁₂ oxo clusters with distinct electrocatalytic activities. Chemical Communications, 2022, 58, 4759-4762.	4.1	4
461	Synthesis and Third-Order Nonlinear Optical Properties of Metal–Organic Zeolites Built from Ti ₄ (embonate) ₆ Tetrahedra. Crystal Growth and Design, 2022, 22, 66-73.	3.0	4
462	Zeolitic metal-biomolecule frameworks based on supertetrahedral lithium clusters and hypoxanthine nucleobase. Inorganic Chemistry Communication, 2016, 71, 82-85.	3.9	3
463	A pair of homochiral porous metal–organic frameworks with a helical metal-carboxylate layer. New Journal of Chemistry, 2016, 40, 1927-1929.	2.8	3
464	Hydrogen bond-assisted homochiral lattice packing between inorganic helices built from heterometallic units. Dalton Transactions, 2018, 47, 2134-2137.	3.3	3
465	Synthesis and Photoelectric Properties of Metal–Organic Zeolites Built from TO ₄ and Organotin. Inorganic Chemistry, 2019, 58, 12521-12525.	4.0	3
466	Understanding the Efficiency and Selectivity of Two-Electron Production of Metalloporphyrin-Embedded Zirconium–Pyrogallol Scaffolds in Electrochemical CO2 Reduction. ACS Applied Materials & Interfaces, 2020, 12, 52588-52594.	8.0	3
467	In Situ Encapsulation of Organic Sulfates in Layered Structures of Zinc and Tris(4-(1H-Imidazol-1-yl)phenyl)amine. Crystal Growth and Design, 2020, 20, 4228-4231.	3.0	3
468	Designable Al ₃₂ â€Oxo Clusters with Hydrotalciteâ€like Structures: Snapshots of Boundary Hydrolysis and Optical Limiting. Angewandte Chemie, 2021, 133, 4899-4904.	2.0	3

#	Article	lF	CITATIONS
469	Asymmetric metal–organic frameworks with double helices for enantioselective recognition. CrystEngComm, 2021, 23, 4748-4751.	2.6	3
470	The Synthesis and Properties of TIPA-Dominated Porous Metal-Organic Frameworks. Nanomaterials, 2021, 11, 2791.	4.1	3
471	Heterometallic Al ₆ Zn ₁₂ nano-plate with π-conjugated ligand: synthesis and nonlinear absorption properties. Chemical Communications, 2021, 57, 12820-12823.	4.1	3
472	Synthesis, Structure, and Light Absorption Behaviors of Prismatic Titanium-Oxo Clusters Containing Lacunary Lindqvist-like Species. Inorganic Chemistry, 2022, 61, 1385-1390.	4.0	3
473	Heterometallic chiral [Mn13Cu8] single-molecule magnets. Dalton Transactions, 2022, , .	3.3	3
474	Efficient access to 1,3,4-trisubstituted pyrroles via gold-catalysed cycloisomerization of 1,5-diynes. Organic and Biomolecular Chemistry, 2022, , .	2.8	3
475	Inorganic acid influenced formation of Ti ₂₆ and Ti ₄₄ oxysulfate clusters with toroidal and capsule structures. Dalton Transactions, 2022, , .	3.3	3
476	Preparation and Visible-Light Response of Salicylate-Stabilized Heterobimetallic Pb–Ti–Oxo Clusters Initiated via Auxiliary Quaternary Ammonium Salts and a Solvent Effect. Inorganic Chemistry, 2022, 61, 5017-5024.	4.0	3
477	Construction and two-dimensional assembly of double-shell Na@Sn ₆ L ₆ 6@Sn ₃ L ₃ clusters through tetrahedral citrate ligands. Chemical Communications, 2022, 58, 5650-5652.	4.1	3
478	Designable Assembly of Atomically Precise Al4O4 Cubane Supported Mesoporous Heterometallic Architectures. Chemical Science, 0, , .	7.4	3
479	Designing Cage-Supported Cluster-Organic Framework for Highly Efficient Optical Limiting. , 2022, 4, 1397-1401.		3
480	Tuning the formations of metal-1,3,5-benzenetricarboxylate frameworks via the assistance of amino acids. Journal of Solid State Chemistry, 2015, 223, 44-52.	2.9	2
481	A pair of 3D homochiral helical metal–organic frameworks with hetrometallic chains constructed by proline derivative ligands. Polyhedron, 2016, 118, 91-95.	2.2	2
482	Organocatalytic enantioselective Diels–Alder reaction between hydroxymaleimides and <i>in situ</i> generated nitrosoalkenes for direct preparation of chiral hemiketals with 1,2-oxazine skeleton. Organic Chemistry Frontiers, 2021, 8, 6215-6219.	4.5	2
483	Chiral Induction in Aluminum Oxo Sulfate Helical Chains. Crystal Growth and Design, 2022, 22, 3954-3960.	3.0	2
484	Synthesis and structural characterization of a dumbbell-like phenylphosphonate-stabilized Ti ₇ –oxide cluster. Acta Crystallographica Section C, Structural Chemistry, 2018, 74, 1248-1251.	0.5	1
485	Synthesis and crystal structures of three metal-organic frameworks based on a triphenylamine-type polycarboxylic ligand. Chinese Science Bulletin, 2016, 61, 1781-1789.	0.7	1
486	Atomically Precise Zr-Oxo and Zr/Ti-Oxo Nanoclusters by Deep Eutectic-Solvothermal Synthesis. Wuli Huaxue Xuebao/ Acta Physico - Chimica Sinica, 2018, 34, 781-785.	4.9	1

#	Article	IF	CITATIONS
487	MAF-41 with intermediate-sized molecular sieving effect for highly selective separation of styrene. Science China Chemistry, 2019, 62, 1265-1266.	8.2	0
488	Rational assembly of metal-oxo clusters into molecular materials <i>via</i> a "wheel mounting― mode. Inorganic Chemistry Frontiers, 2021, 8, 4102-4106.	6.0	0